Benchmarking parameters for remote electrochemical corrosion detection and monitoring of offshore wind turbine structures

Ahuir-Torres JI[*1], Bausch N[2], Farrar A[2], Webb S[1], Simandjuntak S[1]. [1]School of Mechanical and Design Engineering, [2]School of Energy and Electronic Engineering, University of Portsmouth, Anglesea Road, Portsmouth, PO1 3DJ, United Kingdom.

Nash A, Thomas B. Avonwood Developments Ltd, Bournemouth, BH21 7ND, UK

Muna J, Jonsson C, Mathew D. Avanti Communications, London EC4V 6EB, UK

** Correspondence Author: juan.torres@port.ac.uk; Tel: 02392842519 (Ext. 2519).*

Abstract.

The remote location and position of offshore wind turbine structures severely limits the application of in-situ corrosion detection methods such as ultrasonic, acoustic emission and X-Ray. A Real Time Remote Sensing (RTRS) technology can be implemented to provide autonomous detection and monitoring, providing exhaustive and detailed information on the corrosion process. Utilising the concept of Internet of Things (IoT) through the integration with satellite and terrestrial communication network, *iWindCr,* a technology development project funded by the Innovate UK, aims to design a Wireless Sensor Network (WSN) of smart miniaturised sensors for corrosion detection and monitoring of the offshore wind turbine structures.

This paper discusses the rationale and challenges around the *iWindCr* WSN design, particularly in the development of a miniaturised system and in relation to the provision of power and power consumption. The later has led to the selection and the integration of the electrochemical analysis techniques, namely Open Circuit Potential (OCP) and Zero Resistance Ammeter (ZRA) on the sensor interface system. The verification of these techniques for the corrosion detection sensor has resulted in a database consisting of the corrosion parameter outputs or threshold values of metals specific to offshore wind turbine structures, in this case tower, foundation and nacelle (gearbox). The database provides end users with the benchmark that can be used to detect physical changes during the course of corrosion or passive film damage. These parameters are incorporated in the user interface data analytics software, enabling the quantification of corrosion or film damage.

Keywords:

Offshore, wind turbine, corrosion sensor, electrochemical techniques (OCP and ZRA), Wireless Sensor Network (WSN), Real Time Remote Sensing (RTRS), IoT

Nomenclature

E	Potential.
E^o	Standard Potential.
R	Gas Constant (8.314 $J.mol^{-1}.K^{-1}$)
T	Temperature.
n	Number of Electrons transferred in the Corrosion Reaction.
F	Faraday Constant (96485 C/mol).
C_o	The oxidised species concentration.
C_r	The reduced species concentration.
n_o and n_r	Stoichiometric factor of the oxidised species and of the reduced species, respectively.
I_{corr}	Corrosion Current Density.
R_p	Polarization Resistance.
β_c	Cathodic Tafel Slope.
βa	Anodic Tafel Slope.
$Z_{(f)}$	Impedance at a frequency.
f	Frequency.
t	Time.
E_o	Potential Amplitude.
I_o	Current Density Amplitude.
θ	Shift phase.
$R_{(f)}$	Resistance at a Frequency
$C_{(f)}$	Capacitance at a Frequency.
F_{max}	Frequency at Maximum Shift Phase.
I_n	Stable Current Density at certain Number, n of Measurement.
R_n	Noise Resistance.
σ_E	Potential Standard Deviation.
σ_I	Current Density Standard Deviation.
LI	Localised Index used to distinguish the type of corrosion i.e. localised, mixed or uniform
$I_{R.M.S.}$	Root Mean Square of the Current Density
$C.R.$	Corrosion Rate.
M	Molecular Mass.
ρ	Density of the (Oxidised) Material
I_c	Cathodic Current Density.
I_a	Anodic Current Density.
$E_{applied}$	Applied Potential.
ΔE_p	Passive Potential Range.
E_{bp}	Breakage Passive Film Potential.
H	Type of Element.
ζ	Number of Time Constant
SH	Sentry Hole.

CCD	Charge Coupled Devices.
AE	Acoustic Emission.
LW	Lamb Wave.
RFI	Radio Frequency Identification.
OF	Optic Fibre.
POF	Plastic Optical Fibre**.**
MF	Microbending Fibre.
MD	Magnetometer and Dielectric.
LDV	Laser Doppler Vibrometer.
SQID	Superconducting Quantum Interference Device.
MFL	Magnetic Flux Leakage.
FOC	Fibre Optic-Charge.
HI	Holographic Interferometer.
ER	Electrochemical Resistance.
OCP	Open Circuit Potential.
EN	Electrochemical Noise.
EIS	Electrochemical Impedance Spectroscopy.
LRP	Linear Polarisation Resistance.
ZRA	Zero Resistance Ammeter.
PPC	Potentiodynamic Polarization Curve.
PSD	Power Spectrum Density.
ASTM	American Standard of Testing Material.
FED	Federal Standard.
DIN	Deutsches Institut für Normung (German Institute for Standard)
WT	Wind Turbine

Introduction

Wind energy is recognised worldwide as a proven technology to meet increasing electricity demand, with its added attraction of reduced environmental impact. The UK's geographical location makes it ideal for offshore wind energy, accounting for its status as a world leader in the sector (>£21bn estimated invested by 2020, UKTI 2014). [1-4] The design of the offshore wind turbine (WT) structures and the choice of materials for those structures such as the foundation, platform and tower as well as the turbine parts or nacelle (gearbox and generator) must consider the harsh conditions generated from the wind, the weather, the ultraviolet radiation (sunlight) and the marine (ocean wave)/maritime environment that they will be subjected/exposed to. [4-10] Figure 1 defines the onshore and offshore WTs and their components [10] and Figure 2 shows the schematic of the main parts and materials of an offshore WT. [1,4-7,9,11-13]

Due to the harsh maritime environment, corrosion is one of the inevitable and costly issues in the operation and maintenance of the offshore WT. The design basis of the foundation for example suggests that corrosion protection has been designed to a specific industrial standard such as DNV-RP-B401. [10] From the foundation splashzone upwards, the parts are typically coated, whilst the protection under the splashzone is likely to be a combination of coating and sacrificial anodes. Nevertheless, corrosion of weathering steel, a typical material for the foundation, has been reported to be one of the main threats of the structural integrity of the offshore WTs. From the foundation, the connection to the turbine tower is commonly achieved through a transition piece that is used to adjust non-vertically tolerances of installed foundations which is traditionally made of tubular steels. [1,8,11,14,15]

The remote geographical locations and positioning of critical parts of a WT, for example its nacelle (~90-120m hub height) and blades, makes it unique and challenging for the servicing and maintenance. The environment inside the nacelle of the offshore WTs is different to that of the onshore WTs. The ambient temperature inside the onshore WT nacelle, operating for example in the Saharan climate can be in a wide range from -40°C to +55°C. This could be problematic when selecting the materials for example for the electronic equipment to be able to operate in such a range. [16-21] The condition could be worsened for the offshore WT's due to the need for an airtight nacelle unit in order to minimise the inflow of corrosive outer air and other marine corrosive elements (e.g. salt spray or fog). It could lead to an increase in the internal temperature inside the nacelle such as in the generator part, which could go up to 150°C when the cooling system is not adequately installed. [19,22,23] In modern offshore WT nacelle designs, the application of highly corrosive-resistant materials such as for the gearbox, is proposed to withstand such temperatures. [7,13,19,21] The new design also considers the application of gearbox lubricants that contain a certain type of corrosion inhibitor. [8,13,16,17,20,24-26] The application of high temperature materials or coating, ultrasonics and the installation of hot air generators in the nacelle to reduce moisture for corrosion protection are expensive and deemed to be uneconomical. They only prolong the onset of corrosion and its consequences. The nacelle is still always at risk of corrosion from the salty outer-air and the lubricant (e.g. leakages). Robinson, et.al [27] mentioned that the combined total failures of rotors, air brakes and mechanical brakes for example in the case of German's onshore WTs make up for 18% - 22% of the total of subassembly failures. Although the report did not link all failures specifically to

corrosion issues, some when occurring in the offshore WT nacelle under its operating conditions and environment could be initiated and/or accelerated by the corrosion process such as micro-pitting leading to fatigue cracking.

This leads to the requirement of a technology development for a cost-effective end-to-end Non-Destructive Testing (NDT) corrosion detection and monitoring solution for the offshore WTs. [3,8,10,14,22,23,28-30] This solution should look for methods that allow for a continuous monitoring of a system or a system condition by an operator from a remote and safe control room by means of detecting or monitoring physical or electrochemical changes, for example the thickness of the oxide films and discontinuity on the surface of the materials. The changes can potentially be determined through measuring changes in the passive states or the electrochemical states such as potential, current or resistivity of WT parts or materials. Figure 3 illustrates some of the corrosion detection methods/techniques [28,30-42] [30,34,37,39,41,42]. It is therefore important to determine the benchmark or the values of the corrosion parameters and thresholds to identify the changes, which can vary with the detection techniques and materials.

The work reported here is part of the *iWindCr* project, which is a technology development project funded by the Innovate UK. *iWindCr* aims to design a wireless smart miniaturised sensor network (or WSN) for corrosion detection and monitoring. It utilises the concept of Internet of Things (IoT) to integrate the WSN with satellite and terrestrial communication networks, providing a guaranteed Internal Protocol (IP) for data backhaul from the remote wind-farm sites to the control room. By monitoring the backhauled data, the output data can be used as indicators or references for identifying the event and type of corrosion when it takes place.

There are three main parts outlined in this paper. The first part presents a review of many published reports and journals on the main turbine materials and electrochemical analysis techniques. There are indeed many reported works on corrosion detection techniques for various materials and environments but they are not necessarily specific to offshore WTs. This review will therefore focus on materials and electrochemical techniques considered relevant and suitable for the application in offshore WT corrosion detection and monitoring.

The second part discusses the rationales and challenges around the design of the sensor interface system. The challenges are mainly related to the development of a miniaturised system, energy harvesting, and the integration of the two selected electrochemical analysis techniques for corrosion detection and monitoring onto the sensor interface system.

The final part reports the verification programme of the *iWindCr* WSN. One of the outcomes of this programme is the development of a database of electrochemical analysis corrosion parameter outputs or threshold values as a function of materials and environment. The database will benefit the end-users such as wind farm owners or managers and inspectors by providing benchmark data in order to identify the occurrence and type of corrosion. Considering the data scatter and the variability of the data sources, and for the repeatability and reliability of the database, the data are validated. For this purpose, *iWindCr* also includes in its programme the in-house laboratory testing performed to the specification or test conditions and environment as close as to those reported in the literature as well as in compliance to the relevant

international testing standards. Although the in-house laboratory data from testing are included in the data presented here, the verification and validation tests and their outputs will not be discussed in detail as these are outside the scopes of this paper.

Materials for the offshore WT Structures

The offshore WT structure typically comprises of various materials such as polymers, composite, concrete and metallic alloys. [1,11,12,43-49] The majority of the structure is made of one or more metallic components as illustrated in Figure 2 The type of the metal and the kind of alloy vary depending on the size and part of the WT. Aluminium alloys and other light metallic alloys are typically chosen for a small turbine to reduce the cost of the production. While for a large WT, steels are more commonly used to provide the structural strength.

The types of steel used for the tower and the foundation of the offshore WTs are typically structural steels such as weathering steels, also known as atmospheric corrosion resistant steels. The standard BS EN10025 [50] classifies S235, S275, S355, S420, S690 and S890 in relation to the increased yield strength of the steel. The transition piece typically used in a monopole structure is commonly manufactured using steel-flange-reinforced shear panels using stainless steels such as the SS316, which require a lot of welding at the joints. Recently, the high performance compact-reinforced-composite (CRC) has been studied as an alternative to the steel flange for the transition piece material [18,51]. Though stainless steels provide good strength to resist aerodynamic and mechanical loadings.

Towers of small WTs commonly are using the BS-EN573 [49] classified aluminium alloys including the AA 3103, and 5052 because of their good cost-efficiency whilst the larger WT towers comprise more of steel alloys. These alloys will have corrosion protection such as sacrificial anode and/or protective coatings because of their exposure to aggressive environments such as seawater or salt spray, ultraviolet radiation, microorganisms. Details on corrosion prevention methods and protection of wind turbine components can be found in [8,10,15,19,20,24-26,29,30,37,52-55].

The WT materials for the nacelle gearbox and the rotor hub are mainly carbon steels with a small percentage of aluminium and copper alloys. Stainless steels and aluminium alloys that have low wear (scuffing) resistance are not suitable for gears, instead case hardened or chromium-molybdenum alloy steels (18-5 or 17-6 NiCrMo) are used.[16,19,20,29] There is a larger percentage of copper alloys found in the generator because of its good electromagnetic conductivity. The weathering and other carbon steels can be employed in the fabrication of the nacelle bedplate. Since they have low corrosion resistance, they must be protected by means of surface treatments such as epoxy painting or metal-spraying.[1,11,12,24-27]

Stainless steels are traditionally used for the rotor hub and the blades because of the elevated hardness, high corrosion resistance and good mechanical properties. To reduce the weight-to-strength ratio, aluminium alloys of series 2XXX, 3XXX, 6XXX and 7XXX would be a good substitute due to their lightness, acceptable mechanical properties and cost efficiency. [11,46,56,57]

The Aluminium alloys 6XXX are used as an alternative for the blades hub, especially for the smaller WT blades.[27,46] As the turbine design and technology continuously evolve, blades will see the use of composites for example metal matrix composite (MMC) involving steel, Glass-Fiber-Reinforced-Plastic (GFRP) and Carbon-Fibre-Reinforced Plastic (CFRP). [7,18,51,58]

Overview on Corrosion processes and detection methods suitable for offshore WT Structures

Due to their specific operating conditions and exposed environment, the offshore WT structures would be more likely to experience a typical wet corrosion. From the type of attack,[31,32,38,59,60] wet corrosion can be classified as either uniform or localised. The uniform attack is considered less harmful for metallic materials because it commonly generates a non-uniform or loose oxide or passive film that could slow down further corrosion of the bulk material. The uniform corrosion is easily identifiable due to its wide attack area. The localised corrosion is more difficult to detect due to its confined nature on a metal surface and the ability to penetrate deeper through the thickness of the parts producing sharply defined holes. Crevice and pitting are examples of a localised corrosion. Pitting is the most insidious forms of corrosion and when present on clean metal surfaces, it indicates the start of breakdown of passivity and/or of inhibitor-produced protection. Pitting can be even more damaging when hidden under surface deposits, for example under the oxide layers/corrosion products, coating or painting. Pitting can act as an anode and the metal surface acts as a cathode creating a continuous cycle of an active galvanic cell. On fresh surfaces of a metal such as stainless steel with only a few scattered pits, when the ratio of cathode-to-anode area is high, penetration progresses more rapidly causing accelerated localized attacks. This could happen, for example, when the steels are exposed to an oxygenated NaCl electrolyte, from either full immersion in salt water or even from the intermittent salt spray/fog. This is the most common environment of the offshore WTs. Pitting is generally more distributed over the fresh surface with carbon and low alloy steels in relatively moderate corrosion environment. The type of localised corrosion would very much depend on materials, environmental conditions and other factors, such as parts' geometry or interferences with other processes like wear, friction, and fatigue. [32,33,35,38,60-62]

The localised wet corrosion is considered more problematic to the health of the offshore WT structures because they exhibit a higher corrosion rate and are more difficult to detect. Small isolated pits on a generally non-corroded surface are virtually indistinguishable.

There are various methods/techniques that can be used for corrosion detection and monitoring. Commonly they are classified according to the type of signals such as electromagnetic radiation, electric and sonic wave signals. These methods can be further subcategorised depending on the applied signal ranges used for analyses or on the specification of evaluation. A schematic summary of the different corrosion detection and monitoring methods can be seen in Figure 3. [30,34,37,39,41,42] The use of in-situ techniques such as ultrasonic, acoustic emission (AE) or X-Ray among others represented in Figure 3 allows the detection of pitting or other localised corrosion. With regards to detection and monitoring corrosion of a structure in a remote and inaccessible location, these techniques have their limitations. One of which is due

to access for the operator and the power source. [14,28,34] Autonomous techniques and solutions are needed to provide exhaustive and detailed information on the corrosion process that are reliable and cost effective. The application of Real Time Remote Sensing (RTRS) technology would have the means to perform such tasks. [7,8,14,22,23,30,34,39,41,42] This technology utilises a sensor system that can remotely monitor the physical and electrochemical changes. The electrochemical analysis techniques can therefore be adapted onto the sensor system in order to measure the changes for example through the measurements of current, resistance or the electrode potential between the surface of the metals (cathode) and a certain standard reference which could well be another metal (anode, also known as standard electrode). These techniques which include the Open Circuit Potential (OCP), the Electrochemistry Impedance Spectroscopy (EIS), the Zero Resistance Ammeter (ZRA), the Linear Polarisation Resistance (LPR) and the Electrochemical Noise (EN) are briefly discussed as follows in view to determine suitable techniques that can be implemented in a WSN system. [31,32,34,35,38,59,61-67]

The **OCP** is often referred to as the equilibrium potential or the rest potential. It is a non-destructive and passive technique. A passive sensor simply detects and responds to some type of input from the physical environment without the need of external source of power to operate. This method can be used to provide information on the fresh metal corrosion potential which is used as the starting points for the application of electrochemical protection method, to determine the potential distribution on the corroding surfaces that can be used to indicate heterogeneous mixed electrodes and can distinguish whether the corrosion system is in active or in passive state. The OCP method measures the electrode potential, E as a function of temperature and concentration of the oxidised and reduced solutions (see Equation 1).

$$E = E^o + \frac{R \times T}{n \times F} \log \left(\frac{[C_O{}^{no}]}{[C_r{}^{nr}]} \right) \qquad \text{Equation (1)}$$

This method is unsuitable for determining the rate of corrosion because of the non-kinetic and thermodynamics nature of the parameters. The corrosion density current, I_{corr} $(= \frac{E}{R_p})$ can be indirectly evaluated when the polarization resistance, R_p is known. The corrosion reaction is commonly non-ohmic resistance i.e. the increase in current with the electrode potential does not follow a straight line.

The **LRP** is a non-destructive, active technique (requires external power to operate) utilising a Direct Current (DC) or Alternating Current (AC). This technique can be used to identify the two types of corrosion (general/uniform or localised). The corrosion density current, I_{corr} can be evaluated since the LRP measures the changes of the electrode potential and the current density to calculate the polarization resistance, R_p. Their relationships are shown in Equations 2 and 3.

$$R_p = \frac{\Delta E}{\Delta I} \qquad \text{Equation (2)}$$

$$I_{corr} = \frac{B}{R_p} \qquad \text{Equation (3)}$$

$$B = \frac{\beta_c * \beta_a}{2.303 * (\beta_c + \beta_a)} \qquad \text{Equation (4)}$$

The Tafel anodic and cathodic slopes β_a and β_c , respectively are very specific to a certain corrosion process. These slopes can be determined by employing a Potentiodynamic Polarization Curve (PPC) technique, which is categorically a destructive technique. Although the LRP can define the I_{corr} for certain corrosion process, this method is unsuitable for diffusion controlled - corrosion process e.g. for metals with passive film.

The **EIS** is a non-destructive, active technique, which utilises a small amplitude alternating current (AC) signal to probe the impedance characteristics of a cell, which normally constitutes of an anode, a cathode and an electrolyte (electrically conducting solution). The AC signal is scanned over a wide range of frequencies to generate an impedance spectrum for the electrochemical cell under test. This technique allows the study of capacitive, inductive, and diffusion processes taking place in the electrochemical cell and therefore can be used to determine when breakage of the passive film or a localised corrosion has occurred. This technique provides the polarisation resistance R_p as that obtained from the LPR technique and therefore can evaluate the corrosion current density.

Equations 5-7 show the relationships between the impedance, $Z_{(f)}$ as a function of time, t and the polarisation resistance, R_p which is the resistance at the lowest frequency (≤0.01 Hz). Using Equations 3 and 4, the current density can be evaluated.

$$Z_{(f)} = \frac{E_o * \sin(2 * \pi * f * t)}{I_o * \sin(2 * \pi * f * t + \theta)} \qquad \text{Equation (5)}$$

$$\underset{\theta=0}{\Longrightarrow} R_{(f)} = Z_{(f)} = \frac{E_o}{I_o} \qquad \text{Equation (6)}$$

$$\underset{\theta=max}{\Longrightarrow} \frac{1}{C_{(f)}} = 2 * \pi * f_{max} * R_{(f)} = Z_{(f)} = \frac{E_o}{I_o * \sin(\theta)} \qquad \text{Equation (7)}$$

The **ZRA** is a non-destructive and passive electrochemical technique that can measure directly the current density in the corrosion system by only considering the stable current density measurements. This can be statistically calculated using Equation 8.

$$I_{corr} = I_{R.M.S} = \sqrt{\frac{\sum_1^n I_n^2}{n}} \qquad \text{Equation (8)}$$

The **EN** is also a non-destructive and passive technique. This technique is able to differentiate between the general/uniform and localised corrosion. Furthermore, it can identify the distinct kind of localised corrosion, such as inter-granular, pitting or galvanic. The EN technique can provide the same detailed information on the corrosion process or output parameters as those obtained from the ZRA and LPR techniques. Equations 9 and 10 are the equations associated with this technique. $I_{R.M.S}$ can be calculated using Equation 8.

$$R_n = \frac{\sigma_E}{\sigma_I} \qquad \text{Equation (9)}$$

$$LI = \frac{\sigma_I}{I_{R.M.S}} \qquad \text{Equation (10)}$$

With the exception of the OCP, the discussed techniques are able to provide or estimate the corrosion current density, I_{corr}. This parameter could be correlated to the rate of corrosion as represented in Equation 11.

$$C.R = \frac{I_{corr} * M}{F * n * \rho} \qquad \text{Equation (11)}$$

PPC is another electrochemical analysis technique however it is known to be a destructive method. PPC will therefore not be considered as a suitable technique for the *iWindcr* electrochemical sensor. For completeness, this technique is also discussed here. Its corrosion outputs such as the Tafel slopes are however very useful for the corrosion database as previously discussed. This technique is based on the continuous and constant perturbation of the corrosion system potential and the measurement of its current density in parallel. Equation 12 represents the correlation between the electrode potential and the current density.

$$E_{applied} - E_{corr} = \beta_c \log\left(\frac{I_c}{I_{corr}}\right) + \beta_a \log\left(\frac{I_a}{I_{corr}}\right) \qquad \text{Equation (12)}$$

The E_{corr} vs I_{corr} curve generated from the PPC technique can be differentiated into two parts, which are one for the reduction or cathodic reaction and another for the oxidation or anodic reaction. In the cathodic part, the cathodic current density is much higher than anodic current density. In the anodic part the opposite is true. Equations 13 and 14 show their correlations, respectively.

$$E_{applied} - E_{corr} = \beta_c \log\left(\frac{I_c}{I_{corr}}\right) \qquad \text{Equation (13)}$$

$$E_{applied} - E_{corr} = \beta_a \log\left(\frac{I_a}{I_{corr}}\right) \qquad \text{Equation (14)}$$

In addition, PPC can determine the safety or passive potential range, ΔE_p. ΔE_p is the electrode potential range between the E_{corr} and the breakage passive film potential, E_{bp}. The E_{bp} is the applied electrode potential in the anodic part that causes a sudden increase of the anodic current density, I_a.

Designing *iWindCr WSN*: Rationales and Challenges

The *iWindCr* project first must define the user and system requirements for the WSN. The user requirements are based on the Operation and Maintenance (O&M) of the offshore WTs. The O&M varies depending on the type and size of the WTs. Hence it is difficult to come up with

a one-fits-all approach, particularly in relation to positioning, powering and installing the WSN. Many studies on maintenance strategies of the WTs that have been conducted used the historical failures of certain structures/parts as references. From which the approach of many WT operators currently is based on, i.e. to go through maintenance (repair) about two times a year. [44,45,47,68] Due to the cost issue which is typically 5 to 10 times more than those of the onshore WTs, there is a demand of reduced maintenance i.e. frequency and downtime. [17,47,57,68] DOWEC concept, a project funded by NOVEM, the Dutch Agency for Energy and Environment, for example, has proposed a targeted service demand of a visit once per 12-18 months. [47] The downtime is considered to be of 5-10 days, again depending on the location of repairs, the need of deployment and the built of the towers or cranes and the failures. [44,45,68] The *iWindCr* WSN is therefore aiming for a design life of 3-5 years.

One thing that was identified as the main challenge when defining the system requirements is powering the WSN system. Considering the *iWindCr* deployment plan, illustrated in Figure 4 [69], access to and locating a power source for the WSN are relatively difficult. To ensure reliability and safe operation, the Original Equipment Manufacturer (OEM) is normally very specific and strict with respect to the installation and operation of their parts/products. [7,9,11,27,45] Currently, there is no possibility for the WSN system to harvest energy or power from the WT system directly e.g. the generator. It is therefore the *iWindCr* WSN chose for a stand-alone system that would not interfere with the other WT systems or parts that can risk the WT safe and reliable operation. The energy harvesting for example from solar power is considered, especially for the WSN installed on the tower, foundation and blades. However, for the nacelle or gearbox parts that are mainly located in very tight and enclosed spaces, the use of a small battery for space and weight saving is considered to provide enough power to each WSN system node over a defined period of operation (i.e. 3-5 years), which is therefore a feasible option.

The *iWindCr* WSN design therefore focuses on the development of an efficient and reduced power miniaturised system. This design consideration drives the selection and integration of the two passive electrochemical analysis techniques, i.e. the OCP and ZRA for the corrosion detection and monitoring as well as the design of the sensor interface. After several design iteration, the prototype of the sensor interface circuit diagram is shown in Figure 5. Figure 6 lists some of the parts included in the sensor interface circuit. The details of the design and component selection of the sensor interface will however be discussed in a separate publication. Needless to say, the design and component selection of the sensor interface circuit takes into account power requirements for conducting the measurement i.e. taking a number of readings at certain time intervals and for sending the data to the communication gateway that will in turn relay the data to a backend database and finally the user interface, both via satellite. Figure 7 represents one set of data acquisition test results which are used to determine the optimum number of data needed to collect per measurement for the OCP and ZRA analysis. The test was also used to indicate the period for the sensor to conduct one measurement before the system can be sent to sleep (in order to minimise power consumption). The tests showed that stable outputs, in this case the electrode potential, could be obtained by the sensor when using the OCP electrochemical analysis technique with a minimum of 30 readings per one measurement and with the acquisition time approximately of 120 seconds. Figure 7 furthermore indicates the

independency of the outputs to the type of test material. In order to test the reliability of the sensor in relation to data scatter, an assessment using variance or standard deviation was performed. Figure 7 also demonstrates that the SD or variance does not affect the corrosion sensor output. The WSN is currently designed with the capability to collect 40 sensor readings within 120 seconds per measurement. With the current design and power, the WSN could take up to 12 measurements per day.

Corrosion outputs/parameters database

As previously discussed, the electrochemical analysis techniques can be used to determine the occurrence and to identify types of corrosion through the characterisation of their associated corrosion parameters as illustrated in Table 1. The corrosion outputs of the electrochemical analysis techniques have a big dependency on the type of materials and environmental conditions such as temperature, type and pH of the solutions or solvents that the materials are exposed to. The database containing the corrosion outputs/thresholds for various metals typically used in tower, foundation and nacelle parts of offshore WTs are represented in Tables 2 and 3. These data are collated from the literature as well as from the in-house laboratory tests. Only the literature data from the tests performed in accordance with or in compliance to certain industrial or international standards are included. Table 4 lists the relevant standards. These standards allow for obtaining and controlling the known environment conditions such as pH, temperature, and composition of the solvents. These conditions defined in the standards should closely represent the actual conditions in the field, although other factors from the actual operational environment of the turbine components, for example, the direct stress and shear from the loading application may not be taken into account in this case. As part of the *iWindCr* programme, all these literature data are to be verified and validated by performing in-house testing. Having these standards to follow would certainly help these processes i.e. assuring the repeatability and reliability in the data generation.

The database construction of the corrosion parameter outputs or threshold values aims to provide end users with a benchmark for corrosion detection and monitoring purposes. Figure 8 shows a screenshot of the prototype user interface software developed to inform users whether corrosion has been detected for a particular part or structure of the WT. The database will also be integrated in the data analytics of the *iWindCr* user interface. Utilising the OCP and ZRA analysis techniques, as previously discussed, the type of corrosion as well as corrosion rate or remaining life of a monitored component can be determined. The outputs from these two techniques can be used to inform the users when the uniform attack takes place (general corrosion) or when the passive film breaks (localised corrosion). In addition, using the ZRA analysis technique, the measured current can be used to evaluate the rate of material loss due to corrosion. Figure 9 shows the ZRA corrosion current density measurement with time derived from the sensor data reading of a 316 stainless steel after exposure in the seawater environment (pH=8.3) at room temperature. From the measurement, $I_{R.M.S}$ could be determined and the ZRA analysis technique can be used to evaluate the corrosion rate, C.R. (Equation 11). The C.R of the non-corroded and corroded 316SS test sample in this case were estimated to be $2.286.10^{-5}$ cm/year and $1.260.10^{-4}$ cm/year, respectively.

Although in general, the electrochemical analysis techniques and corrosion parameter outputs of structural metals are well published, [53-55,70-77] the reports on electrochemical analysis work directly related to some of the offshore WT foundation and tower materials and their environments are rather difficult to obtain. For example, there was no reference in this related matter on the weathering steel such as S235 or S355 or aluminium alloys 8060 which are commonly used materials in the foundation/tower. It is even rarer to find the published corrosion outputs for the WT nacelle or gearbox materials. The published corrosion parameter outputs of the stainless steel 316 are mainly limited to those obtained from the laboratory testing using seawater environment but not in any other or mixed environments such as seawater in the presence of microorganisms or lubricants. This mixed environment is most likely to be presence inside the nacelle of the WTs.

Conclusion

The work reported in this paper is conducted as part of the *iWindCr* project, supported and funded by the Innovate UK. The *iWindCr* project aims to design a WSN system for autonomous corrosion detection and monitoring of offshore WT structures. This can be achieved through the implementation of Real Time Remote Sensing (RTRS) technology utilising electrochemical sensor as there are limitations with the use of in-situ techniques such as ultrasonic, acoustic emission and X-Ray with regards to the access for operators and to the power source. The electrochemical sensors instead would allow to remotely monitor the physical and electrochemical changes that take place on the metallic materials. The non-destructive and passive electrochemical techniques such as OCP and ZRA are integrated into the sensor interface of the WSN system to measure the electrode potential and current respectively between the component (metal) surfaces with respect to a certain or standard reference (electrode) to indicate when corrosion or breakage of the passive film has occurred. Choosing these passive techniques helps reducing the power requirements. The design of the sensor interface needs to consider carefully its power and current requirements, as this will determine the overall consumption and period of operation.

In addition to the discussion on the main offshore WT materials, this paper presents an overview of the electrochemical analysis techniques including the OCP, EIS and EN. The database of the corrosion parameter outputs and threshold values of the metallic alloys and their relevant environments specific to offshore WTs structures, in this case the foundation, tower and nacelle (gearbox), are presented. The database can be used as a benchmark for the corrosion detection and monitoring by the end-users. In addition, the database is integrated into the data analytics of the *iWindCr* user interface software, which will enable the life prediction of such monitored WT parts/structures to also be included in the software. This paper highlights how limited the current published corrosion data are with respect to metallic materials and environments of the offshore WT parts/structures. The database can also provide guidance for users to enable corrosion detection and monitoring of such complex and diversified structures. Some of the presented literature data are yet to be verified and validated. *iWindCr* has included in its programme these activities as well as extensive and comprehensive electrochemical testing on previously reviewed WT metallic materials.

Although the work reported here mainly focuses on offshore WT structures, the proposed WSN should be feasibly applicable for other engineering structures in other sectors such as oil and gas, marine, automotive and aeronautics.

Acknowledgment

This work was supported by the Innovate UK *iWindCr* Project (Grant Number 103504) and co-funded by our industrial partners Avonwood Development Ltd (Co. No. 02570711) and Avanti Communication Plc (Co. No. 03101607). The authors would also like to acknowledge the Faculty of Technology and the School of Engineering, University of Portsmouth for their support in this work.

References

1. Estate C. A guide to an offshore wind farm. *Power.* 2010:1-70.
2. Government U. UK Offshore Wind: Opportunities for trade and investment. In: Trade DfI, ed. UKTI. 2015.
3. Government U. Overview of Support for the Offshore Wind Industry. In: Government H, ed. https://www.gov.uk/government/publications?official_document_status=command_and_act_papers. 2014.
4. Higgins P, Foley A. The evolution of offshore wind power in the United Kingdom. *Renewable and Sustainable Energy Reviews.* 2014;37:599-612.
5. Burton T, Jenkins N, Sharpe D, Bossanyi E. *Wind energy handbook.* John Wiley & Sons; 2011.
6. Janssen L, Lacal-Arántegui R, Brøndsted P, et al. Scientific Assessment in support of the Materials Roadmap enabling Low Carbon Energy Technologies: Wind Energy. *JRC Scientific and Technical Reports No. EUR.* 2012;25197.
7. Umaya M, Noguchi T, Uchida M, Shibata M, Kawai Y, Notomi R. Wind power generation-development status of offshore wind turbines. *Mitsubishi Heavy Industries Technical Review.* 2013;50(3):29.
8. Pawsey C. Corrosion Protection for Offshore Wind, Prevention and Aftercare: Meet the Industry Players. 4th International Conference Corrosion Protection for Offshore Wind; 2016; Berlin, Germany.
9. Van Bussel G, Henderson A, Morgan C, et al. State of the art and technology trends for offshore wind energy: operation and maintenance issues. Paper presented at: Offshore Wind Energy EWEA special topic conference. 2001.
10. DNVGL-RP-0416. Corrosion protection for wind turbine. *Norway, DNV GL*March, 2016.
11. Ancona D, McVeigh J. Wind turbine-materials and manufacturing fact sheet. *Princeton Energy Resources International, LLC.* 2001;19.
12. Perälä T. Wind Power: the Material Requirements. 2010.
13. Greco A, Sheng S, Keller J, Erdemir A. Material wear and fatigue in wind turbine systems. *Wear.* 2013;302(1-2):1583-1591.
14. Gan T-H, Soua S, Dimlaye V, Burnham K. Real-time monitoring system for defects detection in wind turbine structures and rotating components. Paper presented at: 18th World Conference on Nondestructive Testing. 2012.
15. Black AR, Mathiesen T, Hilbert LR. Corrosion protection of offshore wind foundations. *NACE International: Houston, TX, USA.* 2015.
16. Errichello R, Muller J. *Application requirements for wind turbine gearboxes.* National Renewable Energy Lab., Golden, CO (United States); GEARTECH, Albany, CA (United States);1994.
17. Smolders K, Long H, Feng Y, Tavner P. Reliability analysis and prediction of wind turbine gearboxes. Paper presented at: European Wind Energy Conference and Exhibition 2010, EWEC 2010. 2010.
18. Smaili A, Tahi A, Massfon C. Thermal analysis of wind turbine nacelle operating in Algerian Saharan climate. *Energy procedia.* 2012;18:187-196.
19. Junior VJ, Zhou J, Roshanmanesh S, et al. Evaluation of damage mechanics of industrial wind turbine gearboxes. *Insight-Non-Destructive Testing and Condition Monitoring.* 2017;59(8):410-414.
20. Zhou J. *Investigation of surface engineering and monitoring for reliable wind turbine gearboxes*, University of Birmingham; 2017.

21. Ragheb A, Ragheb M. Wind turbine gearbox technologies. Paper presented at: Nuclear & Renewable Energy Conference (INREC), 2010 1st International. 2010.

22. Zaher A, McArthur S, Infield D, Patel Y. Online wind turbine fault detection through automated SCADA data analysis. *Wind Energy.* 2009;12(6):574-593.

23. Schlechtingen M, Santos IF. Comparative analysis of neural network and regression based condition monitoring approaches for wind turbine fault detection. *Mechanical systems and signal processing.* 2011;25(5):1849-1875.

24. Momber A, Plagemann P, Stenzel V. Performance and integrity of protective coating systems for offshore wind power structures after three years under offshore site conditions. *Renewable Energy.* 2015;74:606-617.

25. Price SJ, Figueira RB. Corrosion Protection Systems and Fatigue Corrosion in Offshore Wind Structures: Current Status and Future Perspectives. *Coatings.* 2017;7(2):25.

26. Weinell CE, Black AR, Mathiesen T, Nielsen PK. New Developments in Coatings for Extended Lifetime for Offshore Wind Structures. Paper presented at: CORROSION 2017. 2017.

27. Robinson C, Paramasivam E, Taylor E, Morrison A, Sanderson E. Study and development of a methodology for the estimation of the risk and harm to persons from wind turbines. *Report, MMI Engineering Ltd, UK.* 2013.

28. BDM Frdral Inc VAM. Corrosion Detection Technologies-A Sector Study. *North American Technology Industrial Base Organization (NATIBO).* March 1998.

29. Zhou J, Roshanmanesh S, Hayati F, et al. Improving the reliability of industrial multi-MW wind turbines. *Insight-Non-Destructive Testing and Condition Monitoring.* 2017;59(4):189-195.

30. Hossain ML, Abu-Siada A, Muyeen S. Methods for Advanced Wind Turbine Condition Monitoring and Early Diagnosis: A Literature Review. *Energies.* 2018;11(5):1309.

31. McCafferty E. Introduction to corrosion science. 2010. *Alexandria: Springer.*

32. Shreir LL. 1.6 - Localised Corrosion. *Corrosion (Third Edition)*. Oxford: Butterworth-Heinemann; 1994:1:151-151:212.

33. Legat A, Dolecek V. Corrosion monitoring system based on measurement and analysis of electrochemical noise. *Corrosion.* 1995;51(4):295-300.

34. Agarwala VS, Reed PL, Ahmad S. Corrosion detection and monitoring-A review. Paper presented at: CORROSION 2000.2000.

35. Jeyaprabha C, Muralidharan S, Venkatachari G, Raghavan M. Applications of electrochemical noise measurements in corrosion studies: A review. *Corrosion Reviews.* 2001;19(3-4):301-314.

36. Yang L. *Techniques for corrosion monitoring.* Southwest Research Institute. Institute of Materials, Minerals, and Mining; 2008.

37. Salas BV, Wiener MS. Techniques for corrosion monitoring. *Corrosion Engineering, Science, and Technology.* 2009;44(2):88.

38. Uhlig HH, Revie RW. *Uhlig's corrosion handbook.* Vol 51: John Wiley & Sons; 2011.

39. Márquez FPG, Tobias AM, Pérez JMP, Papaelias M. Condition monitoring of wind turbines: Techniques and methods. *Renewable Energy.* 2012;46:169-178.

40. Tiburcio C, Castaneda H, Pech-Canul M, Itagaki M. *Electrochemical Techniques and Corrosion Monitoring.* The Electrochemical Society; 2015.

41. de Azevedo HDM, Araújo AM, Bouchonneau N. A review of wind turbine bearing condition monitoring: State of the art and challenges. *Renewable and Sustainable Energy Reviews.* 2016;56:368-379.

42. Martinez-Luengo M, Kolios A, Wang L. Structural health monitoring of offshore wind turbines: A review through the Statistical Pattern Recognition Paradigm. *Renewable and Sustainable Energy Reviews.* 2016;64:91-105.

43. Schleisner L. Life cycle assessment of a wind farm and related externalities. *Renewable energy.* 2000;20(3):279-288.

44. Mertens S. *Section Wind Energy, Faculty Civil Engineering and Geosciences Delft University of Technology, Stevinweg 1, 2628 CN Delft, The Netherlands*: Wind engineering2003.

45. Scheu M, Matha D, Hofmann M, Muskulus M. Maintenance strategies for large offshore wind farms. *Energy Procedia.* 2012;24:281-288.

46. Ravikumar S, Jaswanthvenkatram V, Sohaib SM. Design and Analysis of Wind Turbine Blade Hub using Aluminium Alloy AA 6061-T6. Paper presented at: IOP Conference Series: Materials Science and Engineering. 2017.

47. Van Bussel G, Zaaijer M. Reliability, availability and maintenance aspects of large-scale offshore wind farms, a concepts study. Paper presented at: Proceedings of MAREC. 2001.

48. Wilburn DR. *Wind energy in the United States and materials required for the land-based wind turbine industry from 2010 through 2030.* Virginia: US Department of the Interior, US Geological Survey;2011.

49. Standard B. Aluminium and aluminium alloys. Chemical composition and form of wrought products. Chemical composition and form of products. *EN, BS 573-3:2013.* 2013.

50. Standard B. Hot rolled products of non-alloy structural steels. General technical delivery conditions. *EN, BS 10025-1:2004.* 2004.

51. Nezhentseva A, Andersen L, Ibsen LB, Sørensen EV. Structural Optimization of an Offshore Wind Turbines Transition Pieces for Bucket Foundations. Paper presented at: EWEA OFFSHORE 20112011.

52. Davis JR. *Surface engineering for corrosion and wear resistance.* ASM international; 2001.

53. Moshrefi R, Ghassem Mahjani M, Ehsani A, Jafarian M. A study of the galvanic corrosion of titanium/L 316 stainless steel in artificial seawater using electrochemical noise (EN) measurements and electrochemical impedance spectroscopy (EIS). *Anti-Corrosion Methods and Materials.* 2011;58(5):250-257.

54. Moradi M, Duan J, Du X. Investigation of the effect of 4, 5-dichloro-2-n-octyl-4-isothiazolin-3-one inhibition on the corrosion of carbon steel in Bacillus sp. inoculated artificial seawater. *Corrosion Science.* 2013;69:338-345.

55. Jun C, Zhang Q, Li Q-a, Fu S-l, Wang J-z. Corrosion and tribocorrosion behaviors of AISI 316 stainless steel and Ti6Al4V alloys in artificial seawater. *Transactions of Nonferrous Metals Society of China.* 2014;24(4):1022-1031.

56. Daaland O, Auran L, Furu T, Inventors; Google Patents, assignee. High corrosion resistant aluminium alloy. 2002.

57. Sastri VS. *Challenges in Corrosion: Costs, Causes, Consequences, and Control.* John Wiley & Sons; 2015.

58. Mishnaevsky L, Branner K, Petersen H, Beauson J, McGugan M, Sørensen B. Materials for wind turbine blades: an overview. *Materials.* 2017;10(11):1285.

59. Inman D, Picard G. 2.10 - Corrosion in Fused Salts. *Corrosion (Third Edition)*. Oxford: Butterworth-Heinemann; 1994:2:130-132:142.

60. Schweitzer PA. *Fundamentals of metallic corrosion: atmospheric and media corrosion of metals.* CRC press; 2006.

61. Chen J-F, Bogaerts W. Electrochemical emission spectroscopy for monitoring uniform and localized corrosion. *Corrosion.* 1996;52(10):753-759.
62. Cottis R. Interpretation of electrochemical noise data. *Corrosion.* 2001;57(3):265-285.
63. Gabrielli C, Keddam M. Review of applications of impedance and noise analysis to uniform and localized corrosion. *Corrosion.* 1992;48(10):794-811.
64. Scully JR. Polarization resistance method for determination of instantaneous corrosion rates. *Corrosion.* 2000;56(2):199-218.
65. Kuang F, Zhang J, Zou C, et al. Electrochemical Methods for Corrosion Monitoring: A Survey of Recent Patents. *Recent Patents on Corrosion Science.* 2010.
66. Barsoukov E, Macdonald JR. *Impedance spectroscopy: theory, experiment, and applications.* John Wiley & Sons; 2018.
67. Papavinasam S. Electrochemical Techniques for Corrosion Monitoring. *Corrosion Monitoring Techniques," L. Yang, Ed., Woodhead Publishing, Success, UK.* 2008.
68. Seyr H, Muskulus M. Value of information of repair times for offshore wind farm maintenance planning. Paper presented at: Journal of Physics: Conference Series. 2016.
69. Ahuir-Torres J.I TJ, Currie J, Dawkins D, Jefferies J, Bausch N, Simandjuntak S, Nash A, Thomas B, , Muna J JC, Mathew D. iWindCr solution for corrosion detection and monitoring of offshore wind turbine structures. WindEurope; 2018; Hamburg, Germany.
70. Bonewitz R. An Electrochemical Evaluation of 1100, 5052, and 6063 Aluminum Alloys for Desalination. *Corrosion.* 1973;29(6):215-222.
71. Bonewitz R. An Electrochemical Evaluation of 3003, 3004, and 5050 Aluminum Alloys for Desalination. *Corrosion.* 1974;30(2):53-59.
72. Rowland HT, DEXTER SC. Effects of the sea water carbon dioxide system on the corrosion of aluminum. *Corrosion.* 1980;36(9):458-467.
73. Otero E, Bastidas J, López V. Analysis of a premature failure of welded AISI 316L stainless steel pipes originated by microbial induced corrosion. *Materials and Corrosion.* 1997;48(7):447-454.
74. Arivarasu M, Devendranath Ramkumar K, Arivazhagan N. Corrosion studies of Trimetallic Material in Synthetic Sea Water Environment. *environment.* 2014;9:10.
75. Xin S, Li M. Electrochemical corrosion characteristics of type 316L stainless steel in hot concentrated seawater. *Corrosion science.* 2014;81:96-101.
76. Han G, Jiang P, Wang J, Yan F. Corrosion-wear behavior of 316L stainless steel under different applied potentials. *Industrial Lubrication and Tribology.* 2017;69(2):234-240.
77. Hoseinieh S, Shahrabi T. Influence of ionic species on scaling and corrosion performance of AISI 316L rotating disk electrodes in artificial seawater. *Desalination.* 2017;409:32-46.
78. Xia D-H, Song S-Z, Behnamian Y. Detection of corrosion degradation using electrochemical noise (EN): review of signal processing methods for identifying corrosion forms. *Corrosion Engineering, Science and Technology.* 2016;51(7):527-544.
79. Macdonald DD. Reflections on the history of electrochemical impedance spectroscopy. *Electrochimica Acta.* 2006;51(8):1376-1388.
80. Liu E, Zhang Y, Zhu L, Zeng Z, Gao R. Effect of strain-induced martensite on the tribocorrosion of AISI 316L austenitic stainless steel in seawater. *RSC Advances.* 2017;7(71):44923-44932.

81. Allahar KN, Butt DP, Orazem ME, et al. Impedance of steels in new and degraded ester based lubricating oil. *Electrochimica acta.* 2006;51(8-9):1497-1504.
82. ASTM. Standard Practice for the Preparation of Substitute Ocean Water. *ASTM-D1141*2013.
83. ASTM. Standard Test Methods for Sulfate-Reducing Bacteria in Water and Water-Formed Deposits. *ASTM-D4412.* 2015.
84. ASTM. Standard Test Method for Acid Number of Petroleum Products by Potentiometric Titration. *ASTM-D664* 2017.
85. ASTM. Standard Test Method for Corrosiveness of Lubricanting Fluid to Bimetallic Couple. *ASTM-D6547* 2016.
86. Administration USGS. Corrosiveness and Oxidation Stability of Light Oils. *FED STD-791 Method 5308*. Washington. 1986.
87. ASTM. Standard Test Method for Detection of Copper Corrosion from Lubricanting Grease. *ASTM-D4048* 2016.
88. ASTM. Standard Test Method for Rust-Preventing Characteristics of Inhibited Mineral Oil in the Presence of Water. *ASTM-D665* 2014.
89. ASTM. Standard Practice for Operating Salt Spray (Fog) Apparatus. *ASTM-B117.* 1990.
90. Standard G. Acid Spray Testing *DIN-50021-ESS.* 1988.
91. ASTM. Standard Practice for Modified Salt Spray (Fog) Testing. *ASTM-G85.* 2011.

Figures

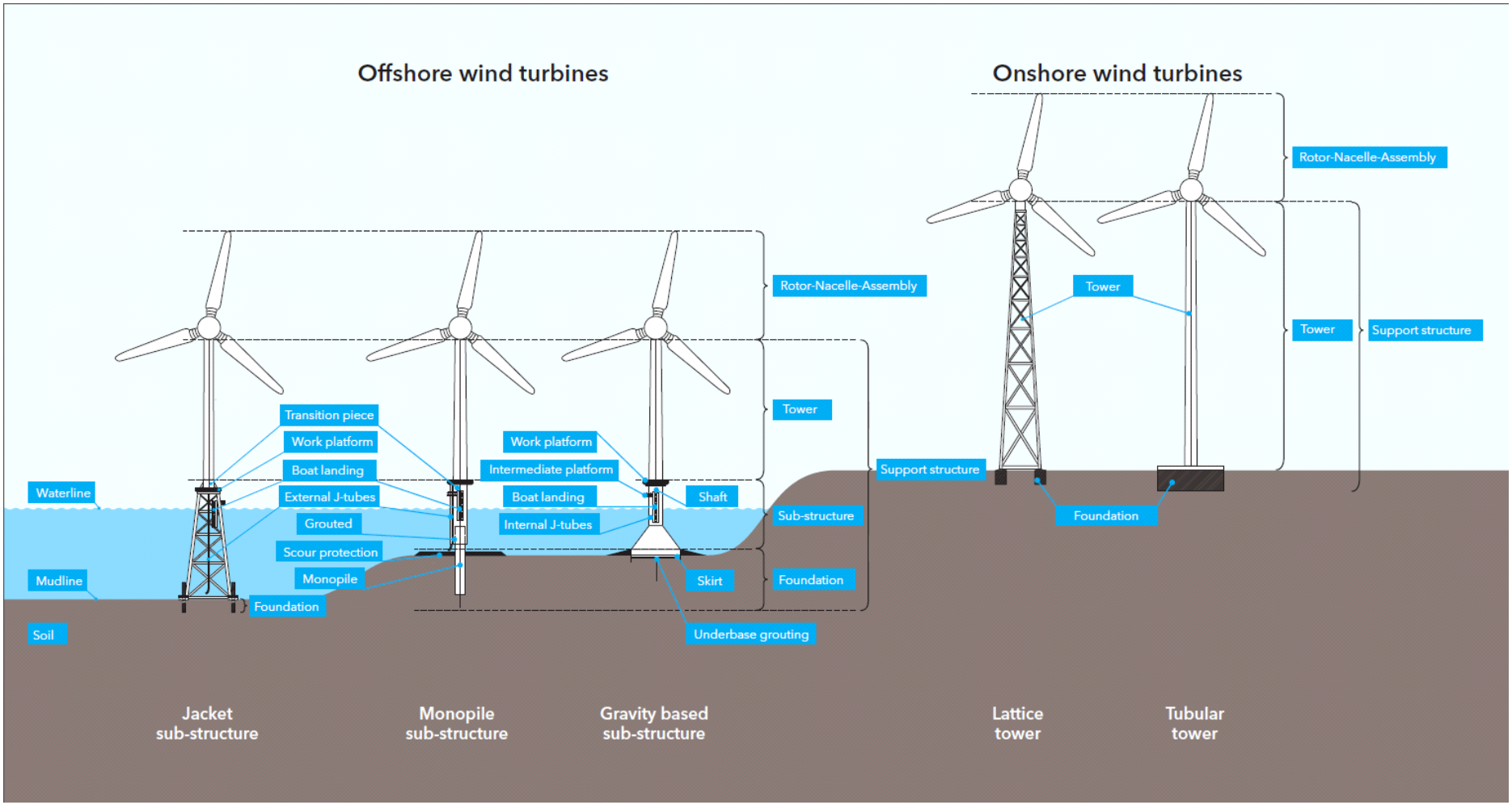

Figure 1: Onshore and Offshore Wind Turbines. [10]

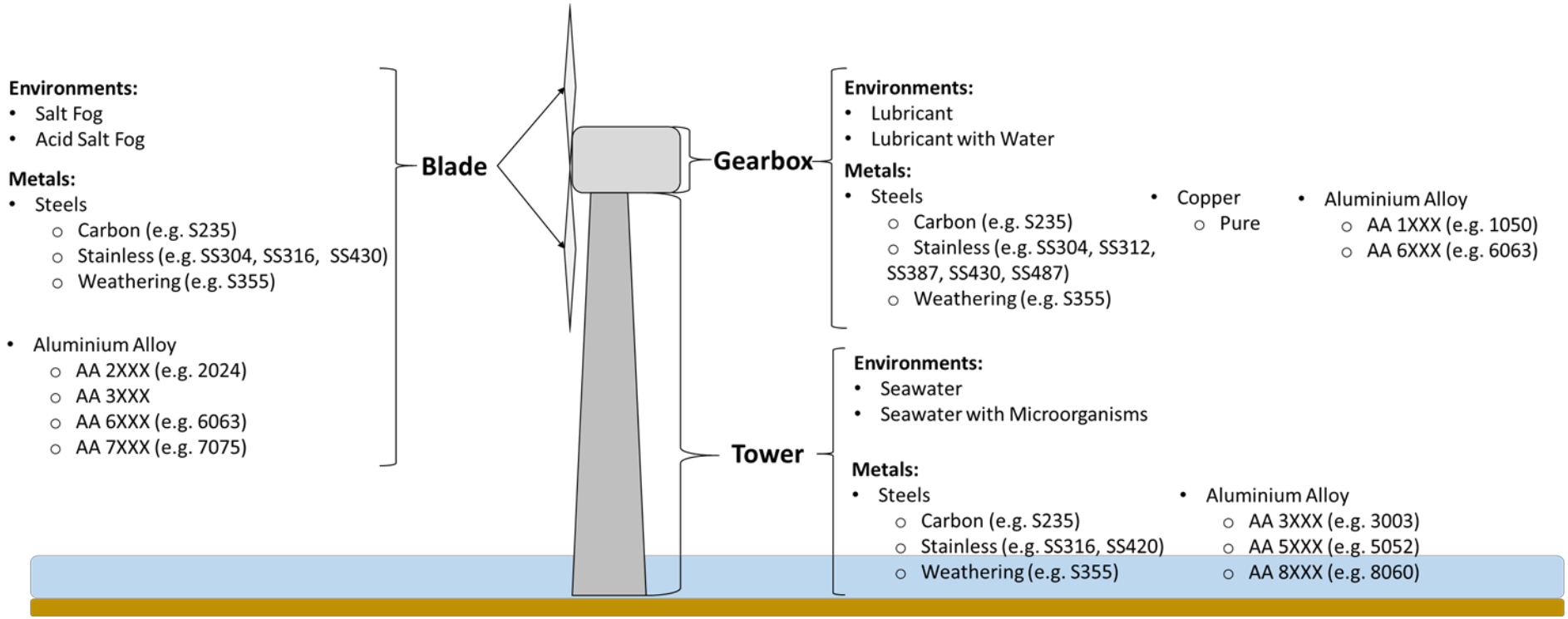

Figure 2: Schematic drawing of the WT parts, metallic materials and environments of the offshore WT.

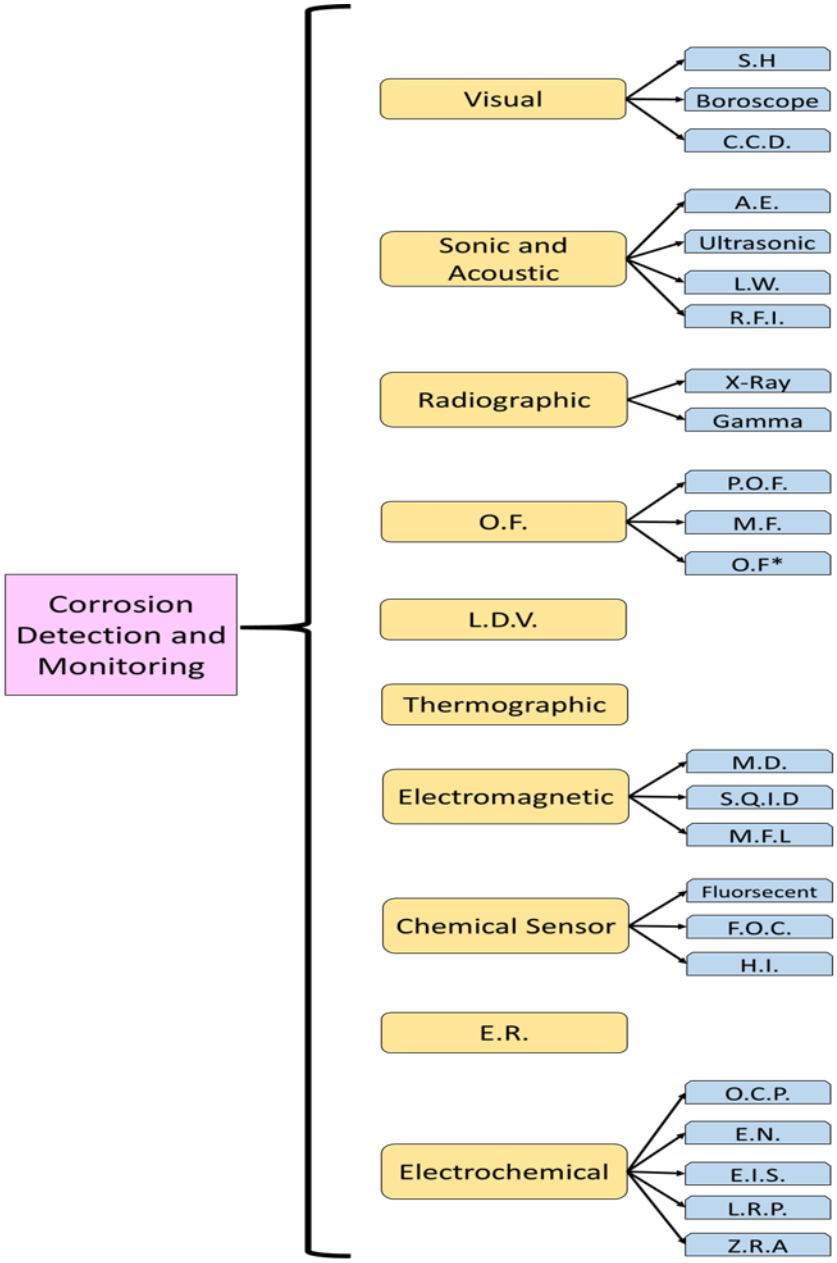

Figure 3: Corrosion detection and monitoring methods/techniques

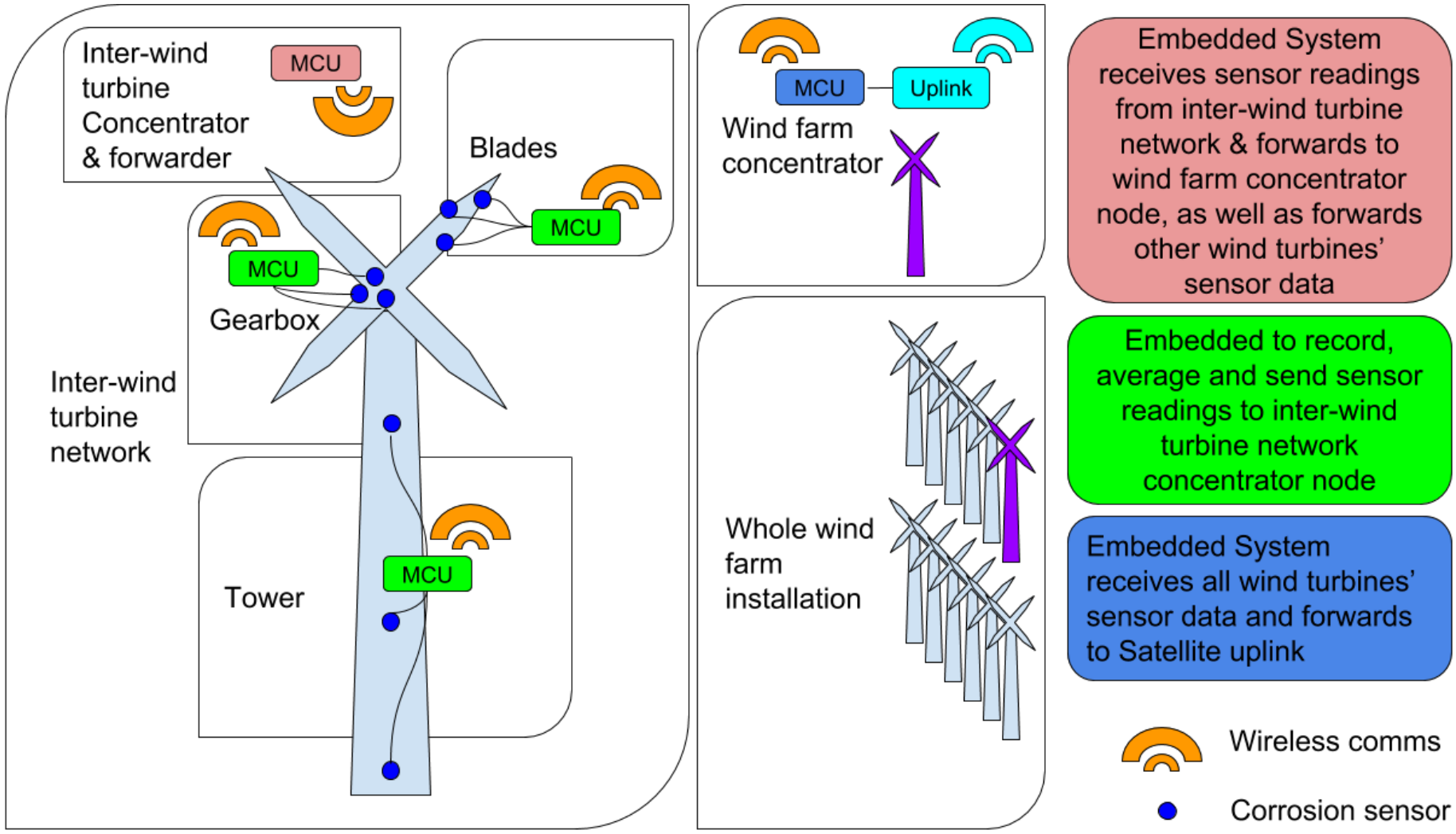

Figure 4: Deployment plan of the *iWindCr* WSN system for corrosion detection and monitoring [69]

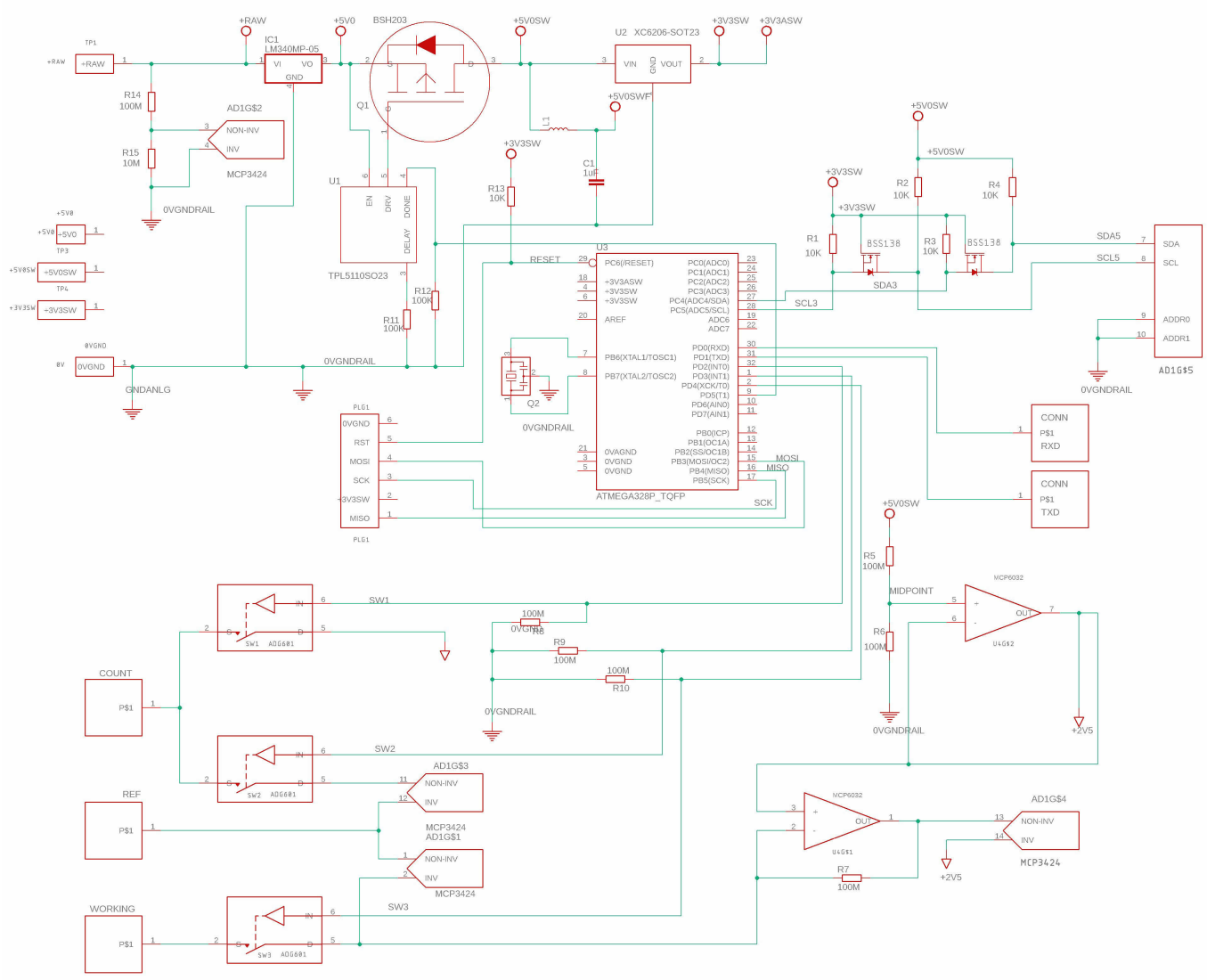

Figure 5: Sensor interface electronic circuit diagram

a. OCP and ZRA Mode Switches
b. Analog to Digital Converter
c. Current to Voltage Converter
d. Quasi Ground 2.5V Reference
e. RS 232 Communication
f. Voltage Level Shifter
g. Power rail switch
h. Voltage Regulator
i. Supply and Supply monitor
j. Nano-timer
k. Ground
l. Programming Port
m. Micro-computer

Figure 6: List of key parts in the sensor interface electronic circuit

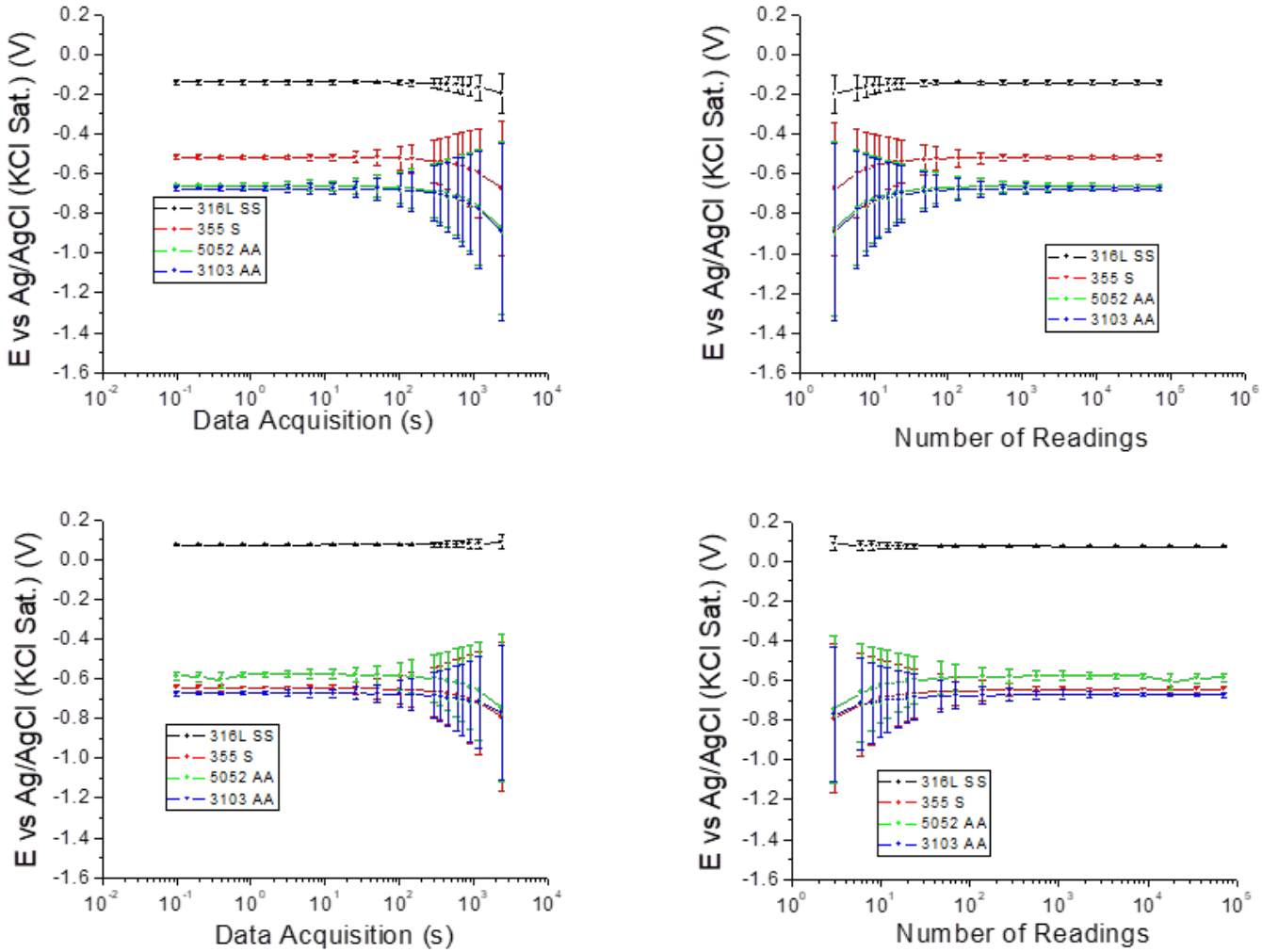

Figure 7: Data acquisition sensor performance testing in seawater at Room Temperature (a)-(b) of non-corroded, (c)-(d) of corroded test samples.

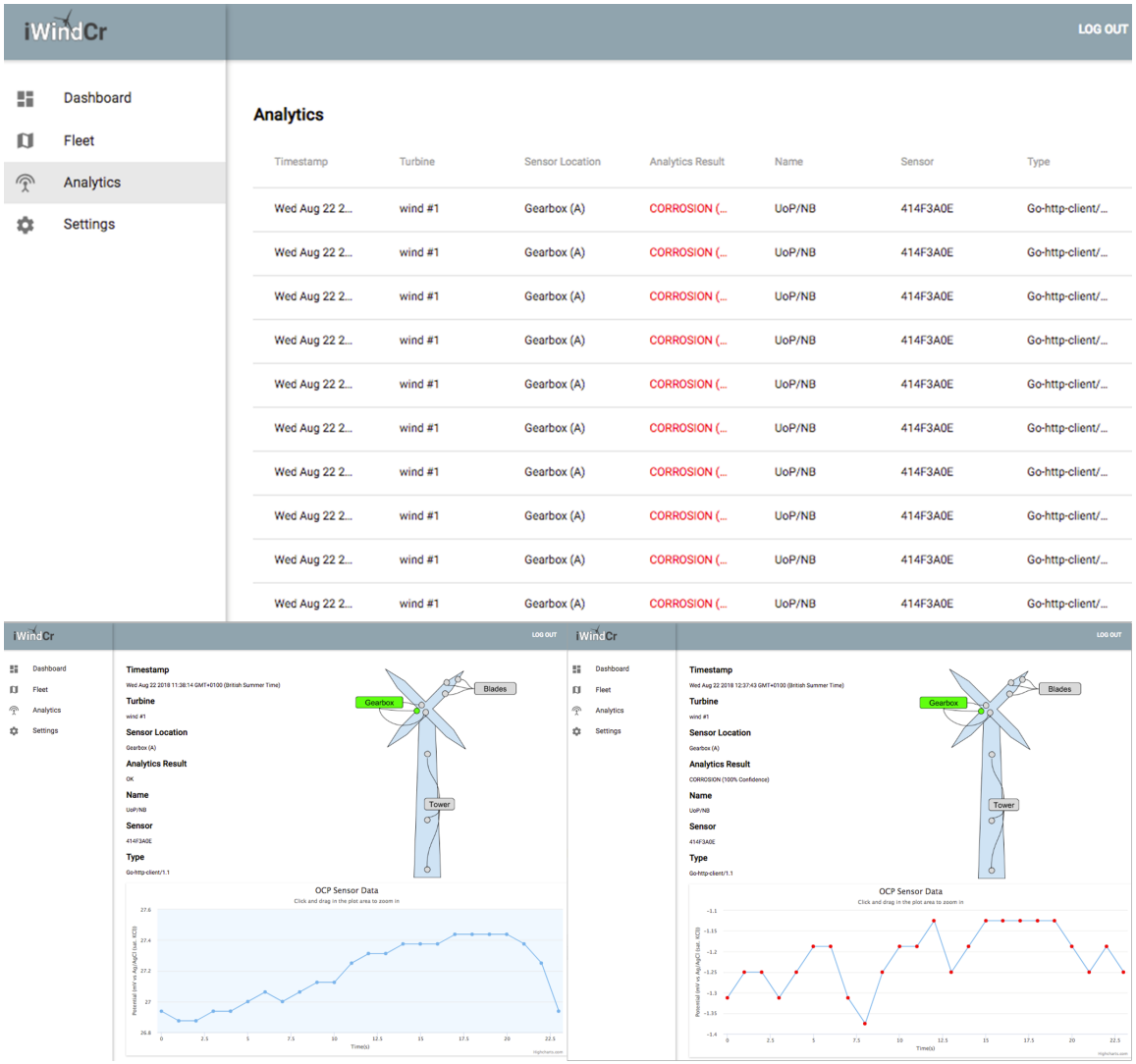

Figure 8. Screenshot of the user interface prototype software

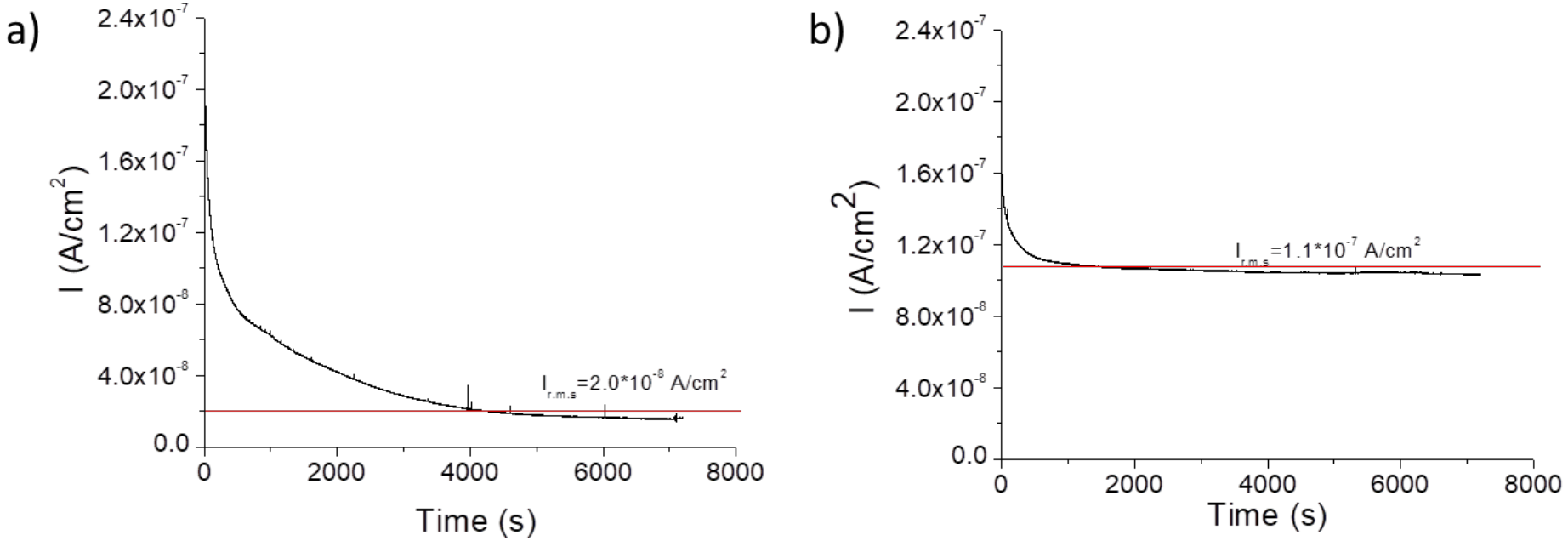

Figure 9. Current density measurements as a function of the time to determine current density root mean square from a) non-corroded and b) corroded 316L Stainless Steel in Seawater.

Tables.

Table 1: Type of corrosion and attack through the characterisation of their associated electrochemical corrosion parameters. [35,62,63,66,78,79]

Type of attack	Type of Corrosion	Output Parameters								
		E^a	$R_n{}^b$	LI^b	PSD^b	$Slope^b$	R^c	C^c	η^c	ζ^c
Uniform/General		X	X	X	X	X	X	X	X	X
Localised	Pitting			X	X	X				
	Galvanic	X	X	X	X	X				
	Inter-granular		X	X	X	X	X	X	X	X
	Exfoliation		X	X	X	X	X	X	X	X
	Hydrogen Embrittlement	X			X	X	X	X	X	X
	Crevice		X	X	X	X	X	X	X	X
	Stress Corrosion Crack		X	X	X	X	X	X	X	X
	Fatigue		X	X	X	X	X	X	X	X
	Fretting	X	X	X	X	X	X	X	X	X
	Microbial	X					X	X	X	X
	Filling		X	X	X	X	X	X	X	X

[a] OCP outputs (E=Electrode Potential)
[b] EN outputs (R_n = noise resistance, LI = Localised Index and PSD = Power Spectrum Density)
[c] EIS outputs (R = resistance, C = capacitance, η = type of element and ζ = number of time constants)

Table 2. Corrosion parameter outputs and threshold values of tower and foundation materials

Environment	Metal	Experimental Conditions	Corrosion Output			
			E^a (V vs Ag/AgCl)			
Seawater (ASTM D1141)	Carbon Steel 235[54]	pH=7 and at 303 K	≥-0.652			
	316 Stainless Steel[55,73,75,76]	pH=8.3 and at 298 K	≤-0.110, ≥0.490			
		Tribological process	≥0.248 Non-sliding, ≥0.046 Sliding			
		Tribological process and at 273 K, 303 K and 333 K	≤-0.310 Non-sliding, ≤-0.560, ≥-0.540 Sliding			
		pH=8.2 and at 345 K	≤-0.120			
	3003 Aluminium Alloy[71,72]	pH=8.2 and at 303 K	≤-0.770			
		pH=8.2 and at 298 K	≤-1.060,≥-0.510			
	5052 Aluminium Alloy[70,72]	pH=7 and at 298 K	≤-0.860≤			
		pH=7.2 and 8.2 at 298 K	≤ -0.660≤ at pH=7.2, ≤ -0.960≤-0.750 at pH=8.2			
	355 Steel[¥]	pH=8.2 and at 298K	≤-0.680,-0.650≤			
	Dissimilar metals Welding, 304, 309 and 434 Stainless Steel[74]	pH=8.2 and at 298K	≤-0.510.≤			
	Dissimilar metals, 316 Stainless Steel and Ti6Al4V[53]	pH=8.2 and at 298K	≤-0.341≤			
Seawater with Microorganims (ASTM D4412)	Carbon Steel 235[54]	*Bacillus sp*	≤-0.472≤			
Seawater (ASTM D1141)	316 Stainless Steel[75,77]	pH=8.3 and, at 298 and at 345K	R^c (Ω*cm^2)	C^c(F/cm^2)	η^c	ζ^c
			<1.42*10^2 <2.65*10^5 (298 K) <10^6 (345 K)	>7.6*10^{-5} >2.2*10^{-5} (298 K)	<0.83 <0.72 (298 K)	1 2 (298 K)
	355 Steel[¥]	pH=8.2 and at 298K	<1.41*10^3 >2.66*10^2 <9.94*10^3	>1.0*10^{-4} <3.6*10^{-4} <9.3*10^{-3}	<0.82 >0.60 >0.16	1 2 3

Environment	Metal	Experimental Conditions	Corrosion Output			
			E^a (V vs Ag/AgCl)			
	5052 Aluminium Alloy¥	pH=8.2 and at 298K	$>3.67*10^3$ $>4.89*10^3$ -	$>1.70*10^{-5}$ $>7.35*10^{-6}$ $<1.01*10^{-3}$	<0.90 <0.91 >0.10	1 2 3
	3103 Aluminium Alloy¥	pH=8.2 and at 298K	$>4.21*10^3$ $>3.78*10^3$ $>3.55*10^4$	$>6.57*10^{-6}$ $>1.27*10^{-5}$ $<1.70*10^{-3}$	<0.93 >0.97 <0.53	1 2 3
	Dissimilar metals, 316 Stainless Steel and Ti6Al4V[53]	pH=8.2 and at 298K	$3.04*10^4$	$8.71*10^{-5}$	N/A	1
Seawater with Microorganims (ASTM D4412)	Carbon Steel 235[54]	*Bacillus sp*	19.28 403.30	$2.01*10^{-3}$ $1.11*10^{-3}$	N/a	1 2
Seawater (ASTM D1141)	Dissimilar metals, 316 Stainless Steel and Ti6Al4V[53]	pH=8.2 and at 298K,	R_n^b ($\Omega*cm^2$)		LI^b	
			$3.68*10^4$		1.05	
	355 Steel¥	pH=8.2 and at 298K	$<1.27*10^2$		>0.04	
	5052 Aluminium Alloy¥	pH=8.2 and at 298K	>67		>0.02	
	3103 Aluminium Alloy¥	pH=8.2 and at 298K	$<3.74*10^2$		>0.06	

¥ Outputs obtained via in house-tests (OCP, EIS and EN) with Ag/AgCl KCl saturated as Reference Electrode and Graphite rod as Counter Electrode.

Table 3. Corrosion parameter outputs and threshold values of gearbox materials.

Environment	Metal	Experimental Conditions	Corrosion Output			
			E^a (V vs Ag/AgCl)			
Seawater (ASTM D114)	316L Stainless Steel[80]	pH=8.2 and Tribological process	≤-0.269, ≥0.489 Non-sliding ≤-0.351/-0.421, ≥0.305 Sliding			
Oil Lubricant (ASTM D6547))	430 Stainless Steel¥	pH=8.8 at 295K and pH=8.2 at 328K	<0.257, >3.000 at 295K <-0.042, >3.000 at 328K			
Grease Lubricant (ASTM D6547))	430 Stainless Steel¥	pH=5.2 and, at 295K	<-0.090, >3.000			
70% (Wt/Wt) Seawater and 30% (Wt/Wt) Grease Lubricant (ASTM D665))	430 Stainless Steel¥	pH=4.3 at 295K and pH=6.8 at 328K	<-0.080, >3.000 at 298K <-0.180, >1.600 at 328K			
Oil Lubricant (ASTM D6547))	235 Steel¥	pH=8.8 at 295K and pH=8.2 at 328K	<1.219, >3.000 at 295K <0.007, >3.000 at 328K			
Grease Lubricant (ASTM D6547))	235 Steel¥	pH=5.2 and, at 295K	<-0.100, >3.000			
70% (Wt/Wt) Seawater and 30% (Wt/Wt) Grease Lubricant (ASTM D665))	235 Steel¥	pH=4.3 at 295K and pH=6.8 at 328K	<-0.120, >3.000 at 298K <-0.160, >3.000 at 328K			
Oil Lubricant (ASTM D6547))	Pure Aluminiumn¥	pH=8.8 at 295K and pH=8.2 at 328K	<-0.190, >3.000 at 295K <-0.250, >3.000 at 328K			
Grease Lubricant (ASTM D6547))	Pure Aluminiumn¥	pH=5.2 and, at 295K	<-0.506, >3.000			
70% (Wt/Wt) Seawater and 30% (Wt/Wt) Grease Lubricant (ASTM D665))	Pure Aluminiumn¥	pH=4.3 at 295K and pH=6.8 at 328K	<-0.650, >0.400 at 298K <-0.680, >3.000 at 328K			
Oil Lubricant (ASTM D6547))	6061-T6 Aluminium Alloy¥	pH=8.8 at 295K and pH=8.2 at 328K	<0.718, >3.000 at 295K <-0.129, >3.000 at 328K			
Grease Lubricant (ASTM D6547))	6061-T6 Aluminium Alloy¥	pH=5.2 and, at 295K	<-0.254, >3.000			
70% (Wt/Wt) Seawater and 30% (Wt/Wt) Grease Lubricant (ASTM D665))	6061-T6 Aluminium Alloy¥	pH=4.3 at 295K and pH=6.8 at 328K	<-0.577, >0.840 at 298K <-0.741, >-0.840 at 328K			
Lubricant (ASTM D664)	434		R^c (Ω*cm^2)	C^c(F/cm^2)	η^c	ζ^c

Environment	Metal	Experimental Conditions	Corrosion Output			
			E^a (V vs Ag/AgCl)			
	Stainless Steel[81]	Non-degraded and Degraded Lubricant	$5.8*10^5$ $1.3*10^7$ $3.5*10^8$ $6.3*10^8$ $6.9*10^4$ $2.2*10^4$	$5.0*10^{-10}$ $2.4*10^{-10}$ $1.0*10^{-10}$ $1.0*10^{-7}$ $5.8*10^{-7}$ $2.8*10^{-4}$		1 2 3 4 5 6
Seawater (ASTM D114)	316L Stainless Steel[80]	pH=8.2 and Tribological process	70 $9.7*10^5$ Non-sliding $4.0*10^5$ Sliding	- $1.1*10^{-5}$ Non-sliding $4.5*10^{-5}$ Sliding		1 2
Oil Lubricant (ASTM D6547))	430 Stainless Steel[¥]	pH=8.8 at 295K and pH=8.2 at 328K	295K $<1.7*10^6$ $>3.8*10^8$ $>4.6*10^6$ 328K $<7.8*10^4$ $<1.9*10^6$ $>6.0*10^4$	295K - $>6.9*10^{-9}$ $<6.2*10^{-11}$ 328K - $>4.8*10^{-6}$ $>6.8*10^{-11}$	295K - >0.57 - 328K - >0.67 -	295K 1 2 3 1 2 3
Grease Lubricant (ASTM D6547))	430 Stainless Steel[¥]	pH=5.2 and, at 295K	$<1.2*10^6$ $<3.0*10^8$ $>6.1*10^6$	- $>3.0*10^{-9}$ $>1.1*10^{-11}$	- <0.77 -	1 2 3
70% (Wt/Wt) Seawater and 30% (Wt/Wt) Grease Lubricant (ASTM D665))	430 Stainless Steel[¥]	pH=4.3 at 295K and pH=6.8 at 328K	295K $<2.6*10^5$ $<7.6*10^7$ $>1.0*10^6$ 328K $<5.7*10^4$ $<1.8*10^6$ $<2.8*10^4$	295K - $>1.7*10^{-8}$ $<3.0*10^{-11}$ 328K - $>4.1*10^{-6}$ $>1.3*10^{-10}$	295K - <1.00 - 328K - >0.74 -	295K 1 2 3 1 2 3
Oil Lubricant (ASTM D6547))	235 Steel[¥]	pH=8.8 at 295K and pH=8.2 at 328K	295K $>4.6*10^5$ $>6.8*10^8$ $>6.2*10^6$	295K - $<1.3*10^{-8}$ $>1.0*10^{-12}$	295K - >0.56 -	295K 1 2 3

Environment	Metal	Experimental Conditions	Corrosion Output			
			E^a (V vs Ag/AgCl)			
			328K $>4.8*10^4$ $<4.5*10^6$ $>3.7*10^4$	328K - $>4.5*10^{-8}$ $<1.1*10^{-10}$	328K - <0.70 -	 1 2 3
Grease Lubricant (ASTM D6547))	235 Steel¥	pH=5.2 and, at 295K	$<1.2*10^6$ $>3.0*10^6$ $<2.1*10^6$	- $<4.0*10^{-8}$ $>6.9*10^{-12}$	- <0.61 -	1 2 3
70% (Wt/Wt) Seawater and 30% (Wt/Wt) Grease Lubricant (ASTM D665))	235 Steel¥	pH=4.3 at 295K and pH=6.8 at 328K	295K $<2.1*10^5$ $<8.9*10^7$ $>1.3*10^6$ 328K $<2.2*10^5$ $<8.0*10^5$ $>1.2*10^4$	295K - $>1.9*10^{-8}$ $>1.9*10^{-11}$ 328K - $>6.6*10^{-7}$ $>3.1*10^{-11}$	295K - 1.00 - 328K - <1.00 -	295K 1 2 3 1 2 3
Oil Lubricant (ASTM D6547))	Pure Aluminiumn¥	pH=8.8 at 295K and pH=8.2 at 328K	295K $>6.0*10^5$ $<4.9*10^8$ $<7.4*10^6$ 328K $>4.2*10^4$ $<2.8*10^6$ $>4.4*10^4$	295K - $>2.8*10^{-9}$ $>9.5*10^{-12}$ 328K - $>2.9*10^{-6}$ $>9.4*10^{-11}$	295K - >0.53 - 328K - >0.63 -	295K 1 2 3 1 2 3
Grease Lubricant (ASTM D6547))	Pure Aluminiumn¥	pH=5.2 and, at 295K	$<3.4*10^6$ $<3.4*10^8$ $>5.0*10^6$	- $>1.8*10^{-8}$ $<6.2*10^{-11}$	- <0.82 -	1 2 3

Environment	Metal	Experimental Conditions	Corrosion Output			
			E^a (V vs Ag/AgCl)			
70% (Wt/Wt) Seawater and 30% (Wt/Wt) Grease Lubricant (ASTM D665))	Pure Aluminiumn¥	pH=4.3 at 295K and pH=6.8 at 328K	295K <3.8*10^5 <3.5*10^7 <2.2*10^6 328K <3.3*10^4 <6.3*10^5 <5.5*10^4	295K - <9.9*10^{-9} <2.2*10^{-12} 328K - <1.3*10^{-6} <1.1*10^{-11}	295K - >0.84 - 328K - >0.72 -	295K 1 2 3 1 2 3
Oil Lubricant (ASTM D6547))	6061-T6 Aluminium Alloy¥	pH=8.8 at 295K and pH=8.2 at 328K	295K >6.0*10^5 <4.9*10^8 <7.4*10^6 328K >3.4*10^4 <4.2*10^6 >7.4*10^4	295K - >2.8*10^{-9} >9.5*10^{-12} 328K - <1.2*10^{-5} >9.0*10^{-11}	295K - >0.53 - 328K - <0.67 -	295K 1 2 3 1 2 3
Grease Lubricant (ASTM D6547))	6061-T6 Aluminium Alloy¥	pH=5.2 and, at 295K	>1.0*10^6 <4.6*10^8 <4.9*10^6	- >1.1*10^{-9} <1.2*10^{-11}	- >0.72 -	1 2 3
70% (Wt/Wt) Seawater and 30% (Wt/Wt) Grease Lubricant (ASTM D665))	6061-T6 Aluminium Alloy¥	pH=4.3 at 295K and pH=6.8 at 328K	295K >3.8*10^5 >7.0*10^7 <2.1*10^6 328K <3.5*10^4 >5.1*10^5 <4.8*10^4	295K - >1.1*10^{-8} >2.0*10^{-11} 328K - >4.3*10^{-7} >1.7*10^{-10}	295K - 1.00 - 328K - <0.96 -	295K 1 2 3 1 2 3
Seawater ASTM D1141	Dissimilar metals, 316 Stainless Steel and Ti6Al4V[53]	pH=8.2 and at 298K,	R_n^b (Ω*cm^2)		LI^b	
			3.68*10^4		1.05	

¥ Outputs obtained via in house-tests (OCP, EIS and EN) with Ag/AgCl KCl saturated as Reference Electrode and Graphite rod as Counter Electrode.

Table.4. List of International/Industrial Standards and Testing Procedures

Issuing Institution	Standard	Title	Environment
ASTM[82]	D1141	Standard Practice of Preparation of Substitute Ocean Water	Seawater
ASTM[83]	D4412	Standard Test Methods for Reducing Bacteria In Water and Water Formed	Seawater with Microorganisms
ASTM[84]	D664	Standard Test Method for Acid Number of Petroleum Products by Potentiometric Titration	Lubricant
ASTM[85]	D6547	Standard Test Method for Corrosiveness of Lubricanting Fluid to Bimetallic Couple.	
FED-STD[86]	791 Method 5308	Corrosiveness and Oxidation Stability of Light Oils	
ASTM[87]	D4048	Standar Test Method for Detection of Copper Corrosion from Lubricanting Grease.	
ASTM[88]	D665	Standard Test Method for Rust-Prevention Characteristics of Inhibited Mineral Oil in the Presence of Water	Mixture of Lubricant with Water
ASTM[89]	B117	Standard Practice for Operating Salt Spray (Fog) Apparatus.	Salt spray/fog
DIN[90]	50021-ESS	Acid Spray Testing	
ASTM[91]	G85	Standard Practice for Modified Salt Spray (Fog) Testing	